Appendix A: derivation of the viscous squeezing force

Squeezing a fluid yields an upwards force. To derive this force, the flow profile of the fluid within the contact needs to be calculated. The derivation of the force coming from the viscosity term of the Navier-Stokes equations is a quite standard procedure [1][2][3]. However, for as far as the authors are aware, the calculation of the viscous force in the specific case of a Power-Law liquid squeezed underneath a spherical piston, does not exist in literature yet. In this Appendix, this force is derived. The inertial part of the Navier-Stokes equations is trickier to include, and therefore this will be ignored in Appendix A, but worked out in Appendix B instead.

To derive the viscous force (and later also the inertial force) the flow profile is retrieved within the gap between surface and piston depicted in Figure 1c. The following definition of dimensionless coordinates and parameters will prove useful later:

$$\tilde{z} \equiv \frac{z}{h} \qquad \text{[A1a]}$$

$$s \equiv \frac{r}{\sqrt{2Rh_0}} \qquad \text{[A1b]}$$

The gap size simplifies in these coordinates to:

$$h = h_0 + \frac{r^2}{2R} = h_0(1 + s^2) \qquad \text{[A2]}$$

and the boundary of pistons surface located at $r = R_s$ is in dimensionless coordinates located at:

$$s_m \equiv \frac{R_s}{\sqrt{2Rh_0}} \qquad \text{[A3]}$$

As is typical for squeeze flow calculations [1], we continue by assuming that the gap size h is very small compared to the characteristic horizontal distance R_s. Therefore, the dominant terms in the $\hat{r}$-projection of the Navier-Stokes equations determine the flow profile. In the defined dimensionless coordinates and by using the Power-Law viscosity model [4], this equation reads:

$$\frac{\partial p}{\partial r} = \frac{K}{h(r)^{1+n}} \frac{\partial}{\partial \tilde{z}} \left(\frac{\partial u_r}{\partial \tilde{z}} \right)^n \qquad \text{[A4]}$$

As normal in the lubrication approximation, it can be assumed pressure does not depend on $\tilde{z}$ as a first order approximation [1][2]. Therefore, the velocity profile $u_r(r, \tilde{z})$ is solved by integrating twice. Using no-slip boundary condition on both the upper and lower surface, solves the integration constants, yielding:

$$u_r(r, \tilde{z}) = \left(-\frac{\frac{\partial p}{\partial r} h(r)}{K} \right)^{\frac{1}{n}} \frac{h(r)}{\left(1+\frac{1}{n}\right)} \left[\left(\frac{1}{2}\right)^{\frac{1}{n}+1} - \left| \frac{1}{2} - \tilde{z} \right|^{\frac{1}{n}+1} \right] \qquad \text{[A5]}$$

Next, the pressure profile is solved by imposing the incompressibility constraint. This implies that the volume of fluid being squeezed out of the gap must be equal to the volume of fluid being expelled by the lowering of the upper surface:

$$2\pi r \int_0^h u_r \, dz = -\pi r^2 \dot{h} \qquad \text{[A6]}$$

The integral is performed, and solving the resulting equation for the pressure term yields:

$$\frac{\partial p}{\partial r} = -2\left(2+\frac{1}{n}\right)^n K\left(-\dot{h}\right)^n \frac{r^n}{h(r)^{2n+1}} \quad [A7]$$

To continue from here, a transition into dimensionless coordinates as defined in Eq.'s A1b and A2 is used. At the boundary $s = s_m$, the pressure must return to ambient pressure, which is defined as zero here, so that the positional integral of Eq. A7 then gives a solution for the pressure:

$$p = 2\left(2+\frac{1}{n}\right)^n K\left(-\dot{h}\right)^n \frac{(2Rh_0)^{\frac{1}{2}+\frac{1}{2}n}}{h_0^{2n+1}} \int_{s_m}^{s} \frac{s^n}{(1+s^2)^{2n+1}} ds \quad [A8]$$

Finally, the viscous force on the piston is given by the integral of the pressure over the entire surface of the piston. The integral is calculated using the dimensionless coordinates:

$$F_v = 2\pi \int_0^{R_s} p(r) r\, dr = 2\pi \cdot 2Rh_0 \cdot \int_0^{s_m} p(s) s\, ds \quad [A9]$$

The viscous force is thus given by:

$$F_v = \frac{K\left(-\dot{h}\right)^n R^{\frac{3}{2}+\frac{1}{2}n}}{h_0^{\frac{3}{2}n-\frac{1}{2}}} X(s_m) \quad [A10]$$

With the function $X(s_m)$ being defined as:

$$X(s_m) = 8\left(2+\frac{1}{n}\right)^n 2^{\frac{1}{2}+\frac{1}{2}n}\pi \cdot \int_0^{s_m} \left[\int_{s_m}^{s'} \frac{s^n}{(1+s^2)^{2n+1}} ds\right] s' ds' \quad [A11]$$

The inner integral in Eq. A11 can only be solved in closed form for specific values of n. For $n = 1$ all integral can be performed and the viscous force returns to the well-known formula for the squeeze of a Newtonian liquid underneath a spherical piston [2][3]:

$$F_v^{n=1} = -\frac{6\pi\eta R^2 \dot{h}}{h_0} \quad [A12]$$

For the calculations displayed in the main manuscript, the function $X(s_m)$ was calculated numerically and tabulated for several values of n, which allowed for quick usage.

As described in the main text, an exact expression for the development of the layer thickness during slow viscous squeezing can be found in literature for the Newtonian case [5]. For more general values of n, the equation of movement

$$m\ddot{h} = F_v \quad [A13]$$

with F_v given by Eq. A10 was solved numerically. This was done by starting with the initial conditions $h_0(t=0) = h_{start}$ and $\dot{h}(t=0) = -v_{start}$ and using the forward Euler method on Eq. A13. For the slow viscous regime this method gives a prediction in agreement with our experimental findings for both PEO 2M (see Figure 2c) as all samples of the more viscoelastic PEO 4M (see Figures A1a and A1b). Note that the values K and n are retrieved from the flow curves of the rheometer measurement, so that no fitting parameters are used in the creation of these curves.

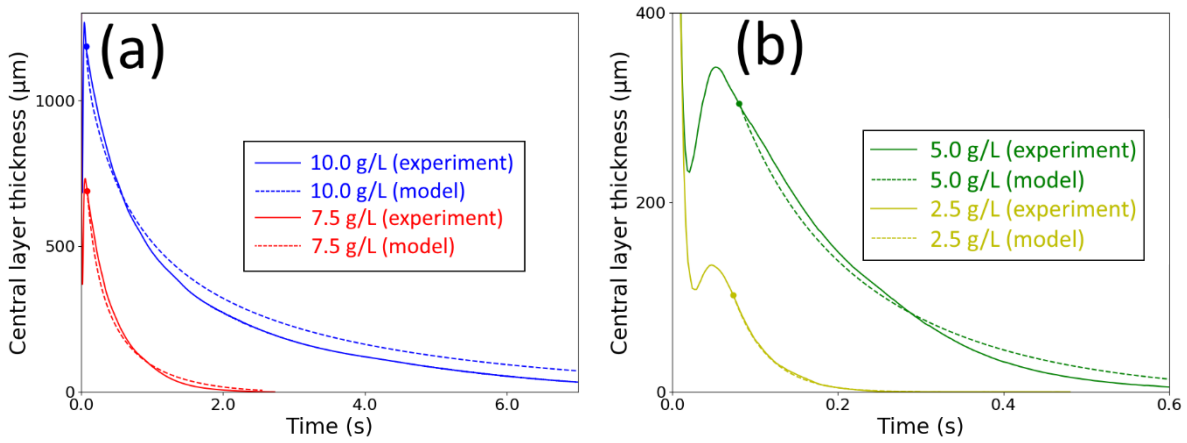

Figure A: The development of layer thickness during the slow viscous squeeze of the viscoelastic liquid PEO 4M with concentrations 10.0 g/L, 7.5 g/L (a) and 5.0 g/L, 2.5 g/L (b). The curves are modeled by Eq. A13 with the dots in the figures corresponding to the starting conditions that are used. The agreement between model and experiment confirms the idea that viscoelastic forces play no role in the slow viscous regime.

References:

[1] J. Engmann, C. Servais and A.S. Burbidge. Squeeze Flow Theory and Applications to Rheometry: A Review. Journal of Non-Newtonian Fluid Mechanics **132**, 1-27 (2005)

[2] A.D. Maude. End Effects in a Falling-Sphere Viscometer. Br. J. Appl. Phys. **12**, 293 (1961)

[3] R.G. Cox and H. Brenner. The Slow Motion of a Sphere Through a Viscous Fluid Towards a Plance Surface – II Small Gap Widths, Including Inertial Effects. Chemical Engineering Science **22**, 1753-1777 (1967)

[4] R.B. Bird, R.C. Armstrong and O. Hassager. Dynamics of Polymeric Liquids, Volume 1: Fluid Mechanics, 2nd Edition. (Wiley, 1987)

[5] A.D. Maude. End Effects in a Falling-Sphere Viscometer. Br. J. Appl. Phys. **12**, 293 (1961)

Appendix B: derivation of the inertial squeezing force

The fluid velocity profile within the gap is harder to find if one includes the inertial terms of the Navier-Stokes equations. Here, we will follow the procedure established by Jackson (1963) and improved by Kuzma (1967), which gives a good estimation for the inertial term. The method was developed for a flat-flat geometry, but a similar derivation for a flat-sphere geometry can be provided following the same steps.

The procedure consists of taking a universal velocity profile $\bar{u}_r$ and $\bar{u}_z$ independent of z, which is substituted into the inertial part of the Navier-Stokes equations. Then, from the viscous term in the Navier-Stokes equations an updated version of the velocity profile is found, which is used to obtain the formulas for pressure and force on the upper surface. Ideally, the updated velocity profile should be substituted back into the inertial part of the Navier-Stokes equations iteratively, leading to a converging scheme for the velocity profile. However, because Kuzma found that only this single iteration already provides a reasonable approximation of the inertial force, we limit ourselves to only substituting the initial universal velocity profile and directly calculate the resulting pressure profile thereafter.

The inertial part of the $\hat{r}$-projection Navier-Stokes reads:

$$\rho\left[\frac{\partial \bar{u}_r}{\partial t} + \bar{u}_r\frac{\partial \bar{u}_r}{\partial r} + \bar{u}_z\frac{\partial \bar{u}_r}{\partial z}\right] = -\frac{\partial p}{\partial r} \qquad \text{[B1]}$$

According to the procedure, $\bar{u}_r$ and $\bar{u}_z$ have been substituted into the left hand side of Eq. B1. Jackson (1963) mistakenly ignored the term $\frac{\partial \bar{u}_r}{\partial z}$, presumably because $\bar{u}_r$ does not depend on z in his analysis. However, Kuzma (1967) performed a more thorough analysis including dependence on z and found that the term $\bar{u}_z\frac{\partial \bar{u}_r}{\partial z}$ contributes equally much to the pressure as the term $\bar{u}_r\frac{\partial \bar{u}_r}{\partial r}$. Because we are here dealing with a spherical upper surface, the dependence of u_z on z is non-trivial to obtain, so precisely repeating Kuzma's steps is non-trivial too. However, we will instead use his observation about the contribution of the described terms, which circumvents the problems with the third term in the left hand side of Eq. B1.

$$\rho\left[\frac{\partial \bar{u}_r}{\partial t} + 2\bar{u}_r\frac{\partial \bar{u}_r}{\partial r}\right] = -\frac{\partial p}{\partial r} \qquad \text{[B2]}$$

From here, we can further continue using the same steps Jackson uses. The average velocity in $\hat{r}$-direction is given by:

$$\bar{u}_r = -\frac{\dot{h}r}{2h} \qquad \text{[B3]}$$

Note that this expression is obtained directly from the incompressibility constrained (see Eq. A6), and it is therefore equally valid for both Newtonian as Non-Newtonian liquids. Whilst taking into account that $\dot{h}$ depends on time, and h depends on both time and position, Eq. B3 is substituted into Eq. B2, yielding:

$$-\frac{\partial p}{\partial r} = \rho\left[-\frac{\ddot{h}r}{2h} + \frac{\dot{h}^2 r}{h^2} - \frac{\dot{h}^2 r^2}{2h^3}\frac{\partial h}{\partial r}\right] \qquad \text{[B4]}$$

The analysis diverges here from [1] and [2], because the curved surface is taken into account now. The parabolic gap profile yields $\frac{\partial h}{\partial r} = \frac{r}{R}$, after which the positional coordinate r is swapped by its dimensionless counterpart s using Eq.'s A1b and A2, yielding:

$$\frac{\partial p}{\partial s} = \rho R \ddot{h} \frac{s}{1+s^2} - 2\rho R \frac{\dot{h}^2}{h_0}\left(\frac{s}{(1+s^2)^3}\right) \quad [B5]$$

Identically to the calculation of the viscous force, at the boundary $s = s_m$ the pressure is assumed to return to ambient pressure, which is defined as zero here. For the two terms in Eq. B5 the integral can be performed, which results into:

$$p = \frac{1}{2}\rho R \ddot{h}\ \log\left(\frac{s^2+1}{s_m^2+1}\right) + \frac{1}{2}\rho R \frac{\dot{h}^2}{h_0}\left(\frac{1}{(1+s^2)^2} - \frac{1}{\left(1+s_m^2\right)^2}\right) \quad [B6]$$

Next, the inertial force is found by integrating the pressure over the surface of the piston, identically to Eq. A9:

$$F_i = -\pi\rho R^2 \ddot{h} h_0 (s_m^2 - \log(1+s_m^2)) + \pi\rho \dot{h}^2 R^2 \frac{s_m^4}{\left(1+s_m^2\right)^2} \quad [B7]$$

Just as in [1] and [2], the inertial force consists of a part that depends on acceleration $\ddot{h}(t)$ and a part that resembles a Bernoulli-like force depending on the velocity squared $\dot{h}^2$. Finally, Eq. B7 can be simplified further if the boundary is assumed to be infinitely far away. For $s_m \to \infty$ the s_m^2 term dominates the acceleration term, and the boundary factor in the $\dot{h}^2$ term becomes 1. By substituting s_m using Eq. A3, it is found that:

$$F_i \approx -\frac{1}{2}\pi\rho R_s^2 R\ddot{h} + \pi\rho R\dot{h}^2 \quad [B8]$$

This formula gives an approximation for the force due to fluid inertia underneath the piston. Using more than one iteration of the procedure described in [1] only updates the factors in front of the terms in Eq. B8 to a better approximation. However, in [1] the next iteration only improves these factors by 20% and there appears to be no reason to believe that for a flat-sphere geometry the improvement by an extra iteration would be significantly different. For the usage in this manuscript, Eq. B8 is therefore sufficiently accurate.

References:

[1] J.D Jackson. A Study of Squeezing Flow. Appl. Sci. Res. 11, 148-152 (1963)
[2] D.C. Kuzma. Fluid Inertia Effects in Squeeze Films. Appl. Sci. Res 18, 15-20 (1967)

Appendix C: solving the fast viscous characteristic differential equation

The characteristic differential equation for fast viscous squeezing is given by:

$$m\ddot{h} = F_v \qquad \text{[C1]}$$

Using the viscous force given in Eq. A10, this equation can be rewritten into:

$$\ddot{h}h_0^{\frac{3}{2}n-\frac{1}{2}} = \left(-\dot{h}\right)^n \frac{KR^{\frac{3}{2}+\frac{1}{2}n}X(s_m)}{m} \qquad \text{[C2]}$$

Given the initial layer thickness X_0 and impact velocity v_0, the following dimensionless parameters are introduced:

$$\tilde{\ddot{h}} \equiv \ddot{h}\frac{X_0}{v_0^2} \qquad \text{[C3a]}$$

$$\tilde{\dot{h}} \equiv \frac{\dot{h}}{v_0} \qquad \text{[C3b]}$$

$$\tilde{h}_0 \equiv \frac{h_0}{X_0} \qquad \text{[C3c]}$$

$$\tilde{t} \equiv t\frac{v_0}{X_0} \qquad \text{[C3d]}$$

$$f \equiv \frac{KR^{\frac{3}{2}+\frac{1}{2}n}X(s_{m\to\infty})X_0^{\frac{3}{2}-\frac{3}{2}n}}{mv_0^{2-n}} \qquad \text{[C3e]}$$

Which turn Eq. C2 into:

$$\tilde{\ddot{h}}\tilde{h}_0^{\frac{3}{2}n-\frac{1}{2}} = \left(-\dot{h}\right)^n \frac{X(s_m)}{X(s_{m\to\infty})}f \qquad \text{[C4]}$$

This equation has to be solved for $\tilde{h}_0(\tilde{t})$ given the initial conditions:

$$\tilde{h}_0(\tilde{t}=0) = 1 \qquad \text{[C5a]}$$

$$\tilde{\dot{h}}(\tilde{t}=0) = -1 \qquad \text{[C5b]}$$

Even for the specific case $n = 1$ and $s_m \to \infty$, a closed form solution of Eq. C4 does not exist [1]. Therefore, it must be solved by numerical means. With the use of an forward Euler algorithm the development of $\tilde{h}_0(\tilde{t})$ has been retrieved. A few examples of this process are shown in Figure 3b in the main text.

It is observed that Eq. C4 reaches a stable value of $\tilde{h}_0(\tilde{t})$ for $\tilde{t} \gg 1$, of which the precise value depends on f. Hence, the fraction of the initial layer left is a function of the parameter f. By running the algorithm over different values of n and f this relation is found, the result of which is shown in Figure 4a in the main text.

In the creation of Figure 4a the assumption $s_m = 0.92$ was used at $\tilde{t} = 0$, according to our experimental conditions. Thereafter, for $\tilde{t} > 0$, s_m was calculated each iteration by using the property that it scales with $\tilde{h}_0^{-½}$.

References:

[1] I.S. Gradshteyn and I.M. Ryzhik. Table of Integrals, Series and Products. (Academic Press, 2015)

Appendix D: derivation of the viscoelastic force by implementation of the Jeffreys model

The Jeffreys model leads to a consecutive relation given by [1]:

$$\boldsymbol{\tau} = -\left(1-\frac{\lambda_2}{\lambda_1}\right)\int_{t'=-\infty}^{t'=t}\frac{\eta_0}{\lambda_1}e^{-\frac{t-t'}{\lambda_1}}\dot{\boldsymbol{\gamma}}(t')dt' - \eta_0\frac{\lambda_2}{\lambda_1}\dot{\boldsymbol{\gamma}}(t) \qquad [D1]$$

Even though the current shear stress now depends on the shear rate $\dot{\boldsymbol{\gamma}}(t')$ of the past, the derivation of the force on the piston follows the same steps as the one for Newtonian squeezing. The flow profile reads:

$$u_r(r,\tilde{z}) = -3\dot{h}\frac{r}{h(r)}\tilde{z}(1-\tilde{z}) \qquad [D2]$$

It must be noted that the dimensional part of this result is directly obtained from the incompressibility constraint (Eq. A6) and not necessarily from the Navier-Stokes equations, and hence Eq. D2 works equally well for the implementation of the Jeffreys model. The parabolic dependency on $\tilde{z}$ is a consequence of the Navier-Stokes equations, but because the no-slip boundary conditions remain applicable, it is reasonable to assume the Jeffreys model implementation does not affect the dependency of u_r on $\tilde{z}$.

The dominant element of $\dot{\boldsymbol{\gamma}}$ to be used in the lubrication approximation is $\dot{\gamma}_{rz}$. Using Eq. D2 it is found that:

$$\dot{\gamma}_{rz} = \frac{\partial u_r}{\partial z} = -3\dot{h}\frac{r}{h(r)^2}(1-2\tilde{z}) \qquad [D3]$$

Using this expression, it follows from Eq. D1 that the shear stress on the top surface at $\tilde{z}=1$ is given by:

$$\tau_{rz} = 3\left(1-\frac{\lambda_2}{\lambda_1}\right)\frac{\eta_0}{\lambda_1}r\int_{t'=-\infty}^{t'=t}\frac{\dot{h}(t')}{h(r,t')^2}e^{-\frac{t-t'}{\lambda_1}}dt' + 3\eta_0\frac{\lambda_2}{\lambda_1}\dot{h}\frac{r}{h(r)^2} \qquad [D4]$$

Substituting the dimensionless s-coordinate in the place of r yields:

$$\tau_{rz} = 3\sqrt{2}\left(1-\frac{\lambda_2}{\lambda_1}\right)\frac{\eta_0}{\lambda_1}\sqrt{Rh_0}s\int_{t'=-\infty}^{t'=t}\frac{\dot{h}(t')}{h_0(t')^2(1+s^2)^2}e^{-\frac{t-t'}{\lambda_1}}dt' + 3\sqrt{2}\eta_0\frac{\lambda_2}{\lambda_1}\frac{\dot{h}}{h_0}\sqrt{\frac{R}{h_0}}\frac{s}{(1+s^2)^2} \qquad [D5]$$

The proximity of the boundary s_m depends on the central layer thickness $h_0(t)$ and hence the coordinate system using s as special coordinate depends on time. Therefore, the factor $\frac{1}{(1+s^2)^2}$ can technically not be taken outside the integral for as long as s_m has changed significantly during the past time λ_1. For computational purposes it is now falsely assumed that s can in fact be taken outside the integral, and upon finding the final result of this derivation, we will discuss the consequences of this decision. The stress can now be written as:

$$\tau_{rz} = 3\sqrt{2}\eta_0\frac{\dot{h}}{h_0}\sqrt{\frac{R}{h_0}}\frac{s}{(1+s^2)^2}M(t,t') \qquad [D6]$$

with $M(t,t')$ a memory function the factor in front of it identical to the shear stress for Newtonian squeeze flow:

$$M(t,t') = \left(1 - \frac{\lambda_2}{\lambda_1}\right)\frac{h_0(t)^2}{\lambda_1 \dot{h}(t)}\int_{t'=-\infty}^{t'=t} \frac{\dot{h}(t')}{h_0(t')^2} e^{-\frac{t-t'}{\lambda_1}}\, dt' + \frac{\lambda_2}{\lambda_1} \quad [D7]$$

From here on forwards, the derivation is identical to that of Newtonian squeeze, with the memory function carried along in each step. Since the memory function contains no coordinate parameters, any integrals over position are unaffected by it. We continue by deriving the pressure distribution with the lubrication approximation $\frac{\partial p}{\partial r} = \frac{\partial \tau_{rz}}{\partial z}$, after which the pressure is integrated over the surface of the upper surface to find the total force, yielding the Newtonian viscous force multiplied by the memory function.

$$F = -\frac{6\pi\eta_0 R^2 \dot{h}(t)}{h_0(t)} \frac{s_m^4}{\left(1+s_m^2\right)^2} M(t,t') \quad [D8]$$

As mentioned before, this result is obtained by neglecting the dependence of the memory function on position. The term $\frac{s_m^4}{\left(1+s_m^2\right)^2}$ is obtained by two separate integrals over s that were only possibly under the assumption that the factor $\frac{1}{(1+s^2)^2}$ in Eq. D5 can be taken in front of the integral-sign. A mathematically better approach would consist of including position into the memory function as well, and integrating over both time and position to obtain the viscoelastic force at a given instance. However, this procedure would be computationally more advanced up to the point that it would provide little extra practical benefit over the thorough analyses of for example Phan-Thien (1987) and Kaushik (2016).

There is however a mathematical trick that allows us to verify that Eq. D8 is a reasonable estimate of the real force predicted by the Jeffreys model. Instead of taking all s *outside* the memory integral, as explained between Eq.'s D5 and D6, we can also take all s *inside* the integral, which would result in the proximity of the boundary term $\frac{s_m^4}{\left(1+s_m^2\right)^2}$ being excluded in Eq. D8 and instead included in the memory function as such:

$$\widetilde{M}(t,t') = \left(1 - \frac{\lambda_2}{\lambda_1}\right)\frac{h_0(t)^2}{\lambda_1 \dot{h}(t)}\int_{t'=-\infty}^{t'=t} \frac{\dot{h}(t')}{h_0(t')^2} \frac{s_m(t')^4}{(1+s_m(t')^2)^2}\, e^{-\frac{t-t'}{\lambda_1}}\, dt' + \frac{\lambda_2}{\lambda_1}\frac{s_m^4}{\left(1+s_m^2\right)^2} \quad [D9]$$

$$\tilde{F} = -\frac{6\pi\eta_0 R^2 \dot{h}(t)}{h_0(t)} \widetilde{M}(t,t') \quad [D10]$$

This would mathematically be an equally false approach as the one used before, but because Eq.'s D8 and D10 denote the two extreme cases (namely taking either all s inside or all s outside the integral) of calculating the force, the real force predicted by the Jeffreys model must be in between. We tested both forms for fitting our experimental data, and we found that both models can replicate the typical viscoelastic 'bump' and that the fitting parameters η_0, λ_1 and λ_2 have the same order of magnitude in both cases. Therefore, we conclude that the choice of taking $\frac{1}{(1+s^2)^2}$ outside of the integral in Eq. D5 has little influence the simulations and that the oversimplified force given in Eq. D8 is actually a good and practical approximation for the range of parameters tested in this manuscript. We used Eq. D8 rather than Eq. D10 to obtain the simulation results discussed in the main text, as intuitively it makes sense that the force should be proportional to the piston surface area πR_s^2 at any given instance.

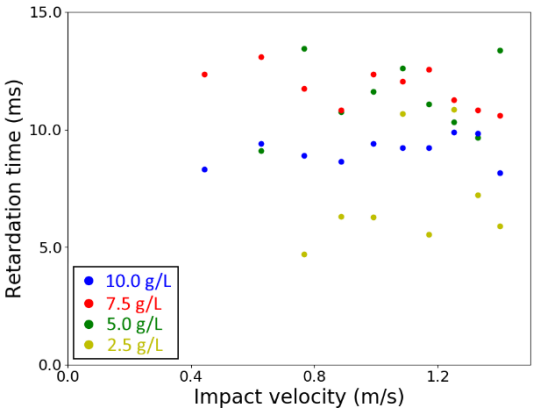

Figure D: The fitted retardation time λ_2 for impact measurements as a function of impact velocity with four different concentrations of PEO (4M). The fitting results for the viscosity η_0 and relaxation time λ_1 can be found in respectively Figures 6d and 6e in the main text.

References:

[1] R.B. Bird, R.C. Armstrong and O. Hassager. Dynamics of Polymeric Liquids, Volume 1: Fluid Mechanics, 2nd Edition. (Wiley, 1987)

[2] N. Phan-Thien, F. Sugeng and R.I. Tanner. The Squeeze-Flim Flow of a Viscoelastic Fluid. Journal of Non-Newtonian Fluid Mechanics **24**, 97-119 (1987)

[3] P. Kaushik, P.K. Mondal and S. Chakraborty. Flow Dynamics of a Viscoelastic Fluid Squeezed and Extruded between Two Parallel Plates. Journal of Non-Newtonian Fluid Mechanics **227**, 56-64 (2016)